ACS OMEGA

http://pubs.acs.org/journal/acsodf

Article

Experimental Study on the Polymer/Graphene Oxide Composite as a Fluid Loss Agent for Water-Based Drilling Fluids

Jingyuan Ma, Shaocong Pang, Zenan Zhang, Boru Xia, and Yuxiu An*

Cite This: *ACS Omega* 2021, 6, 9750−9763

Read Online

ACCESS | Metrics & More | Article Recommendations

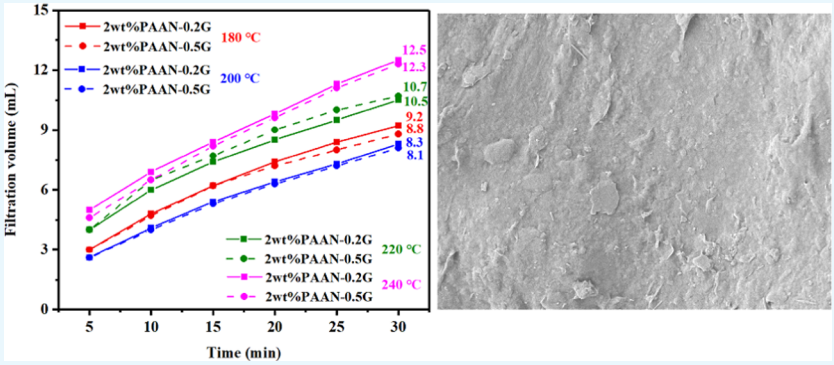

ABSTRACT: The wellbore instability caused by the penetration of drilling fluids into the formation is a vital problem in the drilling process. In this study, we synthesized a polymer/graphene oxide composite (PAAN-G) as a fluid loss additive in water-based drilling fluids. The three monomers (acrylamide (AM), 2-acrylamide-2-methyl-1-propane sulfonic acid (AMPS), *N*-vinylpyrrolidone (NVP)) and graphene oxide (GO) were copolymerized using aqueous free radical polymerization. The composition, micromorphology, and thermal stability properties of PAAN-G were characterized by Fourier transform infrared (FT-IR) spectroscopy and thermogravimetric analysis (TGA). According to the American Petroleum Institute (API) standards, the influence of PAAN-G on the rheological and filtration properties of bentonite-based mud was evaluated. Compared with PAAN, PAAN-0.2G has more stable rheological properties at high temperatures. The experimental results showed that even at a high temperature of 240 °C, PAAN-G can still maintain a stable fluid loss reduction ability. In addition, PAAN-G is also suitable for high-salt formations; it can still obtain satisfactory filtration volume when the concentration of sodium chloride (NaCl) and calcium chloride ($CaCl_2$) reached 25 wt %. Besides, we discussed the fluid loss control mechanism of PAAN-G through particle size distribution and scanning electron microscopy (SEM).

1. INTRODUCTION

The success of drilling operations greatly depends on the performance of the drilling fluids.[1,2] As the essential component in the oil and gas drilling process, drilling fluids are responsible for suspending and transporting cuttings, balancing the formation pressure, cleaning the wellbore, cooling and lubricating drilling tools, and other important functions.[3−5] Good rheological and filtration properties are necessary conditions for drilling fluids to maintain the above basic functions. Various drilling fluids have been developed for different drilling conditions, such as water-based drilling fluids, oil-based drilling fluids, synthetic-based drilling fluids, etc. Among them, water-based drilling fluid has become the most widely used drilling fluid due to its simple preparation, low cost, and environmental friendliness.[6,7] Water is one of the most important components in water-based drilling fluids, precisely because of the large amount of water content that causes various problems encountered in the use of water-based drilling fluids. Water intrusion into the formation will cause many problems, such as formation pollution, shale hydration and swelling, and formation collapse.[8−10] At the same time, the thick filter cake formed on the borehole wall due to the water and particulate invasion can easily lead to problems such as borehole damage and stuck drilling.[11,12] The use of fluid loss additives can slow down the loss of water to the formation. The ideal fluid loss agent should have the characteristics of significantly reducing the fluid loss volume and forming a thin and dense filter cake.[3,13] Besides, as drilling is carried out in

Received: January 20, 2021
Accepted: March 19, 2021
Published: March 30, 2021

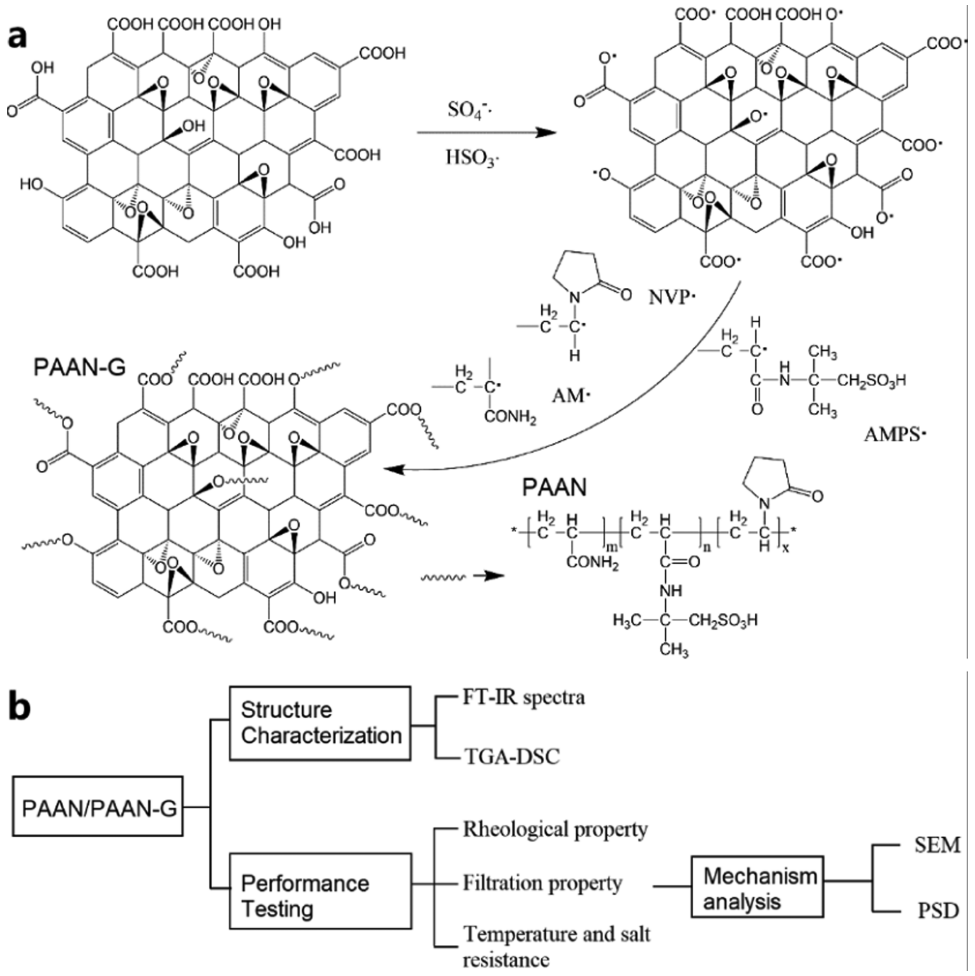

Figure 1. (a) Reaction scheme of free radical polymerization of the acrylamide polymer/graphene oxide composite (PAAN-G); (b) procedure for the characterization of PAAN-G.

deep formations and downhole conditions are becoming increasingly complex, the fluid loss agent should also have the ability to maintain performance in high-temperature and high-salt environments.[14]

Various natural and synthetic polymers have been applied to improve the filtration property of drilling fluids, including xanthan gum,[15] wild Jujube pit powder,[16] tea polyphenols,[17] starch,[18−20] cellulose,[21,22] synthetic polymers,[13,23−26] cationic copolyelectrolyte,[27] etc. Natural polymers, as fluid loss agents, are always easy to degrade at high temperatures, which leads to their failure.[28,29] With the development of nanotechnology, nanomaterials are gradually being studied to reduce the fluid loss of drilling fluids. Nanoparticles have an excellent ability to improve the performance of drilling fluids. For example, block pores and throats improve the rheological properties and reduce filtration volume.[30−32] Cai et al. showed that using cheap unmodified and commercially available silica nanoparticles to formulate water-based drilling fluids can significantly prevent water from invading shale formations.[33] The research of Sensoy et al. showed that when the size of nanoparticles and the pore size of the formation are properly matched, the fluid intruding into the formation will be significantly reduced.[34] In recent years, with the increase in the depth and difficulty of drilling formations, high-temperature and high-salt environments have brought severe challenges to polymers used as rheological control and fluid loss treatment agents. The research of Zhang et al. showed that the type and concentration of salt solution have a great influence on the chain structure of polyacrylamides.[35] Seright et al. proposed that the stability of acrylamide polymers would decrease in the presence of dissolved oxygen and divalent cations.[36] The instability of the polymer seriously affects the stability of the drilling fluid. Therefore, it is necessary to consider improving the stability of the polymer in a high-temperature and high-salt environment. Nanomaterials have the advantages of high surface energy, rigidity, and dimensional stability. Mao et al. prepared an acrylamide polymer-based silica nanoparticle composite material, which has excellent thermal stability, rheology, fluid loss reduction, and lubricity.[37] An et al. grafted acrylamide polymer on the surface of nanosilica to improve the salt tolerance of the polymer.[38] The single-walled carbon nanotubes/poly(vinylpyrrolidone) (SWCNTs/PVP) nanocomposites developed by Rana et al. can significantly improve the instability of shales.[39] The polypropylene−silica nanocomposite (PP−SiO_2NC) studied by Oseh et al. is superior to partially hydrolyzed polyacrylamide in terms of controlling rheology and fluid loss.[40] It can be seen that polymer/nanocomposites can combine the toughness of polymers and the rigidity of inorganic materials, making them more suitable for applications in drilling fluids in complex environments.

https://doi.org/10.1021/acsomega.1c00374
ACS Omega 2021, 6, 9750−9763

Graphene materials have been extensively studied in many fields due to their unique atomic structure and properties.[41,42] Kosynkin et al. first proposed the use of graphene oxide (GO) as a highly effective fluid loss control agent for water-based drilling fluids.[43] They pointed out that an extremely low fluid loss volume can be achieved when the combined ratio of large-flake GO and powdered GO was 3:1. An et al. used graphene modified with ethylenediamine to block micro−nano pores, allowing the drilling fluid to obtain the lowest filtration volume under certain conditions.[44] Aramendiz et al. evaluated the potential of using silica nanoparticles (SiO_2-NPs) and graphene nanosheets (GNPs) to formulate nanoparticle water-based drilling fluids. The results show that when the total concentration of nanoparticles is 0.75 wt % (0.5 wt % of SiO_2-NPs and 0.25 wt % of GNPs), the filtration volume is the lowest.[45] The above studies confirmed the potential of graphene in improving the filtration property of drilling fluids. However, the problem of large additions and high cost limits the use of graphene as a fluid loss agent in drilling fluids.

We are committed to preparing a fluid loss control agent for drilling fluids that can withstand temperatures exceeding 200 °C and can be used stably in high salt concentrations. In this study, we prepared an acrylamide polymer/graphene oxide composite (PAAN-G); the grafting of acrylamide polymer on the surface of graphene oxide not only exerts the toughness of the polymer but also combines the advantages of graphene and greatly reduces the amount of graphene used. We investigated its suitability and potential performance as a fluid loss additive for water-based drilling fluids. At the same time, we evaluated the temperature resistance and salt (sodium chloride and calcium chloride) resistance of PAAN-G.

2. RESULTS AND DISCUSSION

2.1. Characterization of PAAN and PAAN-G. The acrylamide polymer/graphene oxide composite (PAAN-G) was polymerized by the redox system of ammonium persulfate and sodium sulfite, and the polymerization mechanism is shown in Figure 1a. The primary free radicals formed by the decomposition of the initiator cause the hydrogen atoms on the surface of GO to be taken away to generate free radicals, and then carry out chain propagation polymerization with monomers AM, 2-acrylamide-2-methyl-1-propane sulfonic acid (AMPS), and *N*-vinylpyrrolidone (NVP) to finally obtain the composite material of acrylamide polymer grafted GO. Subsequently, the structure and performance of PAAN-G were characterized according to the characterization procedure shown in Figure 1b.

The functional groups on GO were determined by the analysis of the Fourier transform infrared (FT-IR) spectra of GO. Figure 2 shows the FT-IR spectra of GO, PAAN-0.2G, and PAAN. In the FT-IR spectrum of GO, 1733 cm^{-1} was assigned to the C═O stretching vibration, 1288 cm^{-1} was the absorption peak of C−O−C, 3220 cm^{-1} was the absorption peak of −OH, and the skeletal vibration of unoxidized C═C bond and the C−O in the carboxylic acid were seen at 1648 and 1041 cm^{-1}, respectively.[46] In the FT-IR spectrum of PAAN-G, 1654, 1544, and 1290 cm^{-1} were the characteristic absorption peaks of amide I (C═O), amide II (N−H), and amide III, respectively; 1186, 1039, and 628 cm^{-1} were all characteristic absorption peaks of sulfonic groups ($-SO_3H$). PAAN-G and PAAN have extremely similar FT-IR spectra because of the extremely low concentration of GO. However, it can still be seen from Figure 2 that, compared with PAAN, the

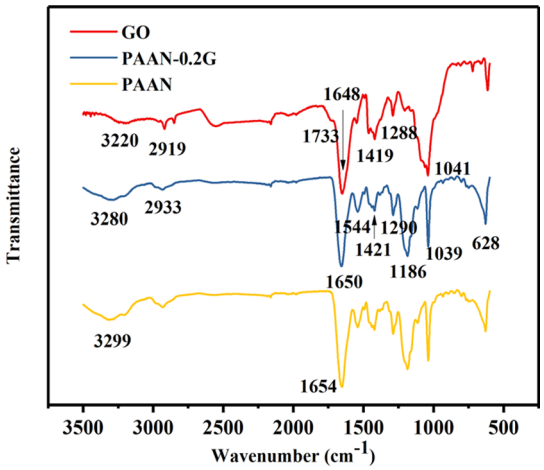

Figure 2. FT-IR spectra of GO, PAAN-G, and PAAN.

absorption peaks of N−H and C═O of PAAN-G shifted to smaller wavelengths, which can prove the formation of hydrogen bonds between GO and PAAN.[46]

The thermogravimetric analysis (TGA) and differential thermal analysis (DSC) curves of GO, PAAN, and PAAN-G are shown in Figure 3, which were used to determine the changes of thermal stability of the synthesized GO composite (PAAN-G) compared with GO and PAAN. GO was thermally unstable and lost about 10% of its weight at 180 °C and about 90% of its weight at 192 °C. This was related to the pyrolysis of the unstable oxygen-containing functional groups to produce carbon monoxide, carbon dioxide, and steam.[47] After compositing with the polymer PAAN, PAAN-G greatly improved the thermal stability of GO and only lost 6% weight at 200 °C, which was caused by the residual free water and bound water in PAAN-G. Compared with PAAN, the thermal stability of PAAN-G was only slightly improved, and the main reason was that the content of GO in the composite was too low. Therefore, the difference in the glass transition temperature and melting temperature between PAAN-G and PAAN was negligible.

2.2. Rheological Properties. Figure 4 shows the comparison of rheological parameters of the base slurry containing PAAN, PAAN-0.2G, and PAAN-0.5G at different temperatures. The viscosity and yield point of the base slurry were extremely low. Although the concentration of clay particles in the base slurry increases due to the high-temperature dispersion, which caused the viscosity and yield point of the base slurry to increase slightly at high temperatures, it was still significantly lower than that in the base slurry after adding the polymer. It can be seen that, compared with the base slurry without additives, 1.0 wt % PAAN, 1.0 wt % PAAN-0.2G, and 1.0 wt % PAAN-0.5G can all increase the viscosity of the base slurry. The good rheological properties required for the drilling fluid are to have lower plastic viscosity and higher yield point because it was difficult to pump the drilling fluid with high PV, and the too low YP was not conducive to suspending and transporting cuttings. It can be seen from Figure 4 that, at room temperature, PAAN-0.2G has more suitable PV and YP values than PAAN. After aging at 150 and 180 °C, the rheological parameters of PAAN, PAAN-0.2G, and PAAN-0.5G have all decreased, but it can be seen that the rheological parameters of PAAN-0.2G changed more slowly. Table 1 lists the change rates of rheological

https://doi.org/10.1021/acsomega.1c00374
ACS Omega 2021, 6, 9750−9763

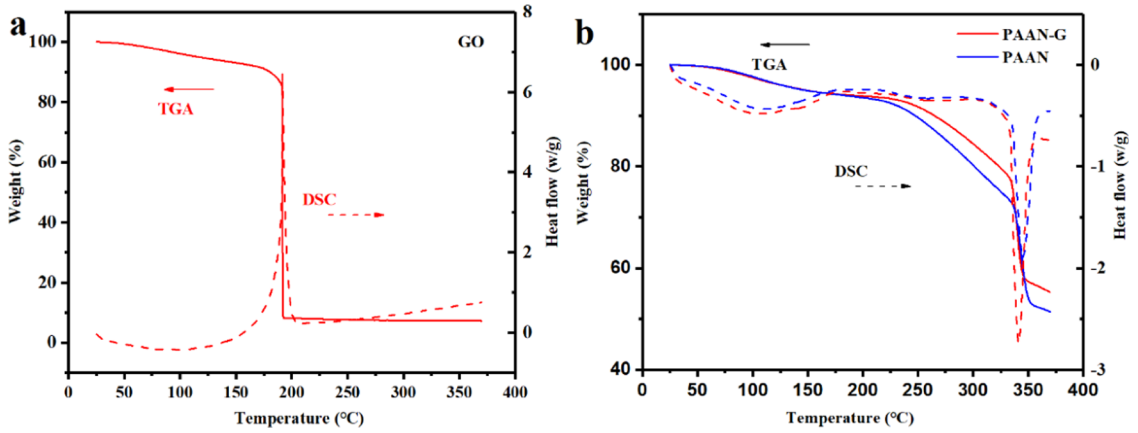

Figure 3. TGA–DSC curves of (a) GO and (b) PAAN and PAAN-G.

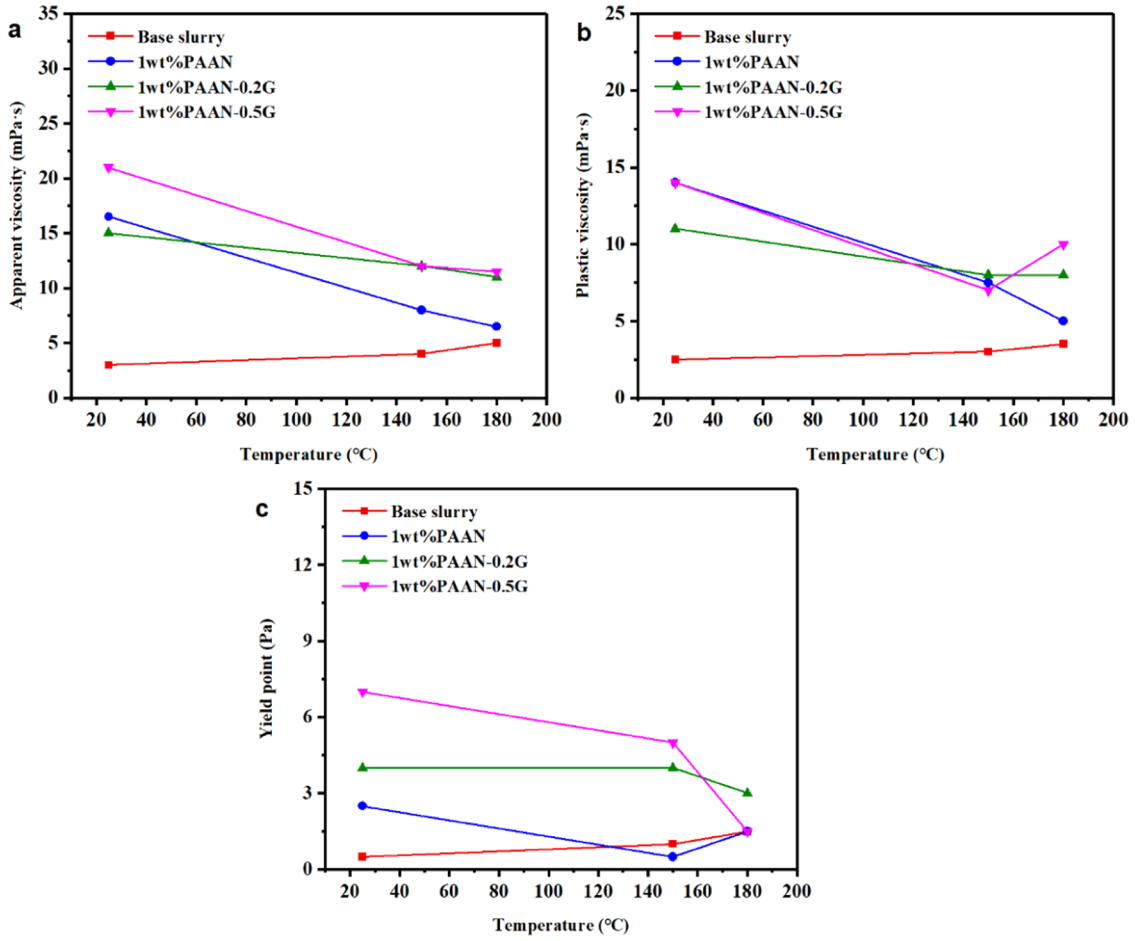

Figure 4. Comparison of rheological parameters of the base slurry and the base slurry containing 1.0 wt % PAAN, 1.0 wt % PAAN-0.2G, and 1.0 wt % PAAN-0.5G at different temperatures: (a) AV, (b) PV, and (c) YP.

Table 1. Change Rate of Rheological Parameters after Aging at 150 and 180 °C

	1 wt % PAAN		1 wt % PAAN-0.2G		1 wt % PAAN-0.5G	
	150 °C (%)	180 °C (%)	150 °C	180 °C (%)	150 °C (%)	180 °C (%)
AV	51.5	60.6	20%	26.6	42.8	45.2
PV	46.4	64.3	27.2%	27.2	50.0	28.6
YP	80.0	40.0	0	25.0	28.6	78.6

parameters of the base slurry containing 1.0 wt % PAAN, 1.0 wt % PAAN-0.2G, and 1.0 wt % PAAN-0.5G after aging at 150 and 180 °C. Whether it was aged at 150 or 180 °C, the reduction rate of AV, PV, and YP of 1.0 wt % PAAN-0.2G was not higher than 28%, while the change rate of rheological parameters of 1.0 wt % PAAN was much higher than that of 1.0 wt % PAAN-0.2G; moreover, its YP reduction rate reached 80% at 150 °C and indicated that the rheological properties of PAAN-0.2G at high temperature were more stable, which is necessary for high-temperature drilling fluids. Compared with

https://doi.org/10.1021/acsomega.1c00374
ACS Omega 2021, 6, 9750–9763

PAAN-0.2G and PAAN, the stability of PAAN-0.5G at high temperature was between the two. Table 2 lists the YP/PV of

Table 2. YP/PV of the Drilling Fluid at Different Temperatures

temperature (°C)	1 wt % PAAN	1 wt % PAAN-0.2G	1 wt % PAAN-0.5G
25	0.18	0.36	0.50
150	0.07	0.50	0.70
180	0.30	0.38	0.15

the base slurry containing different additives at different temperatures. This value reflected the carrying capacity index of the drilling fluid. A higher YP/PV value is conducive to effective rock breaking at high shear rates and effective rock debris carrying capacity at low shear rates.[25] It can be seen from Table 2 that PAAN-G was more conducive to obtaining high YP/PV values than PAAN. In addition, PAAN-0.2G was better than PAAN-0.5G because PAAN-0.2G can still maintain a suitable YP/PV value at 180 °C, while PAAN-0.5G did not. The comparison of rheological properties showed that the polymer-grafted graphene oxide composite (PAAN-G) can effectively improve and stabilize the rheological properties of drilling fluids, no matter at high temperatures or low temperatures, which was significantly different from the ordinary polymer without grafting graphene oxide (PAAN).

2.3. Filtration Properties. The influence of PAAN and PAAN-G on the filtration property of the base slurry is shown in Figure 5. Compared with the base slurry, 1.0 wt % PAAN, 1.0 wt % PAAN-0.2G, and 1.0 wt % PAAN-0.5G can all significantly reduce the API filtration volume. However, the 30 min filtration volume of PAAN-G was lower than that of PAAN. As the aging temperature increased, the difference in the API filtration volume between PAAN-G and PAAN became more obvious. The 30 min API filtration volume of PAAN-0.2G before aging was only 1.4 mL less than that of PAAN, but after aging at 150 and 180 °C, the difference increased to 4.4 and 7 mL. This phenomenon demonstrated that PAAN-G has a better fluid loss reduction effect than PAAN at high temperatures. Based on the comparison of the rheological and filtration properties of PAAN, PAAN-G can maintain stable rheology and fluid loss reduction ability at high temperatures, that is, PAAN-G was more suitable for use at high temperatures than PAAN.

Figure 6 shows the photos and scanning electron microscopy (SEM) images of fresh filter cakes of the base slurry containing 1.0 wt % PAAN or 1.0 wt % PAAN-0.2G after aging at 180 °C. It can be seen from the fresh filter cake photos (Figure 6a,b) that the filter cake formed by PAAN was thicker than that of PAAN-0.2G, and the thick filter cake may cause downhole accidents such as diameter reduction. From the SEM image magnified 1000 times (Figure 6c,d), it can be seen

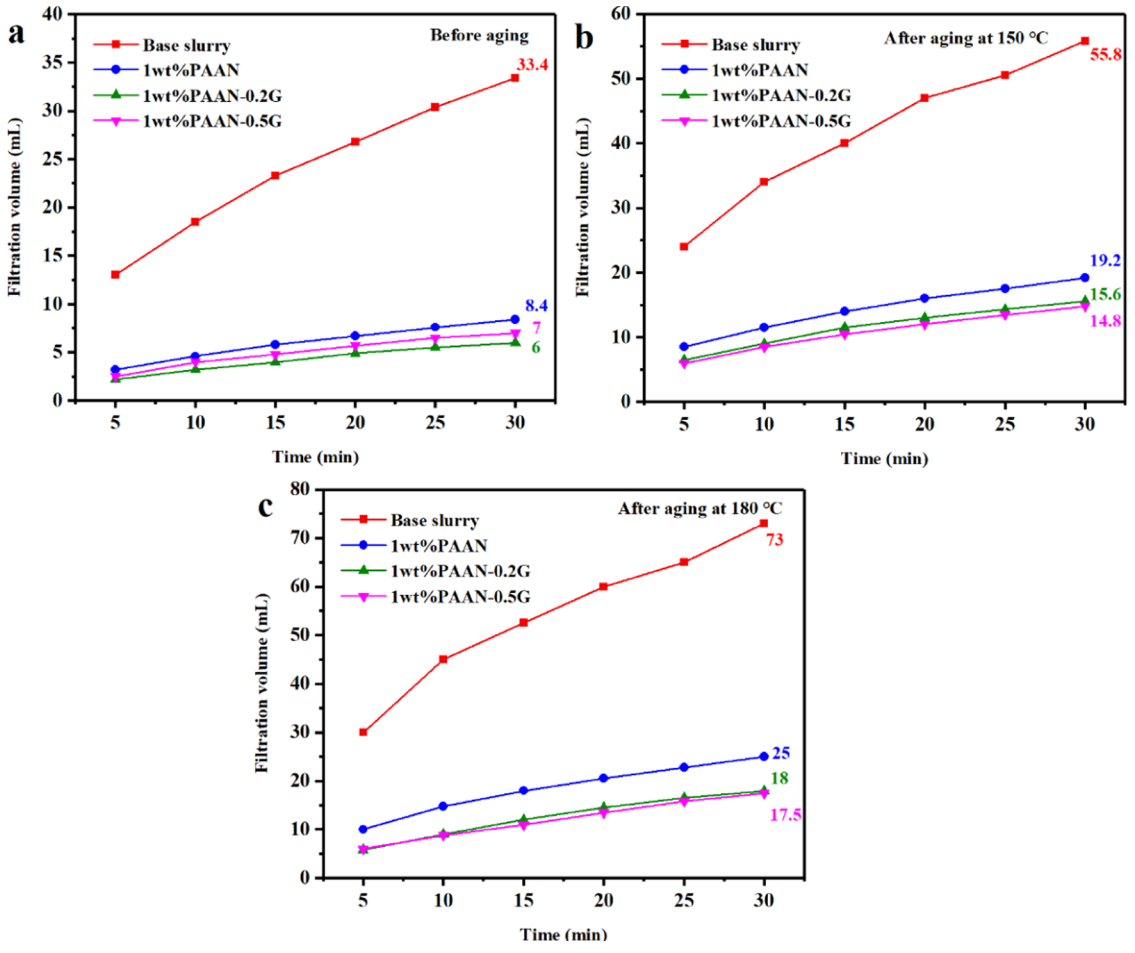

Figure 5. Comparison of the API filtration volume of the base slurry and the base slurry containing 1.0 wt % PAAN, 1.0 wt % PAAN-0.2G, and 1.0 wt % PAAN-0.5G at different temperatures: (a) before aging, (b) after aging at 150 °C, and (c) after aging at 180 °C.

https://doi.org/10.1021/acsomega.1c00374
ACS Omega 2021, 6, 9750−9763

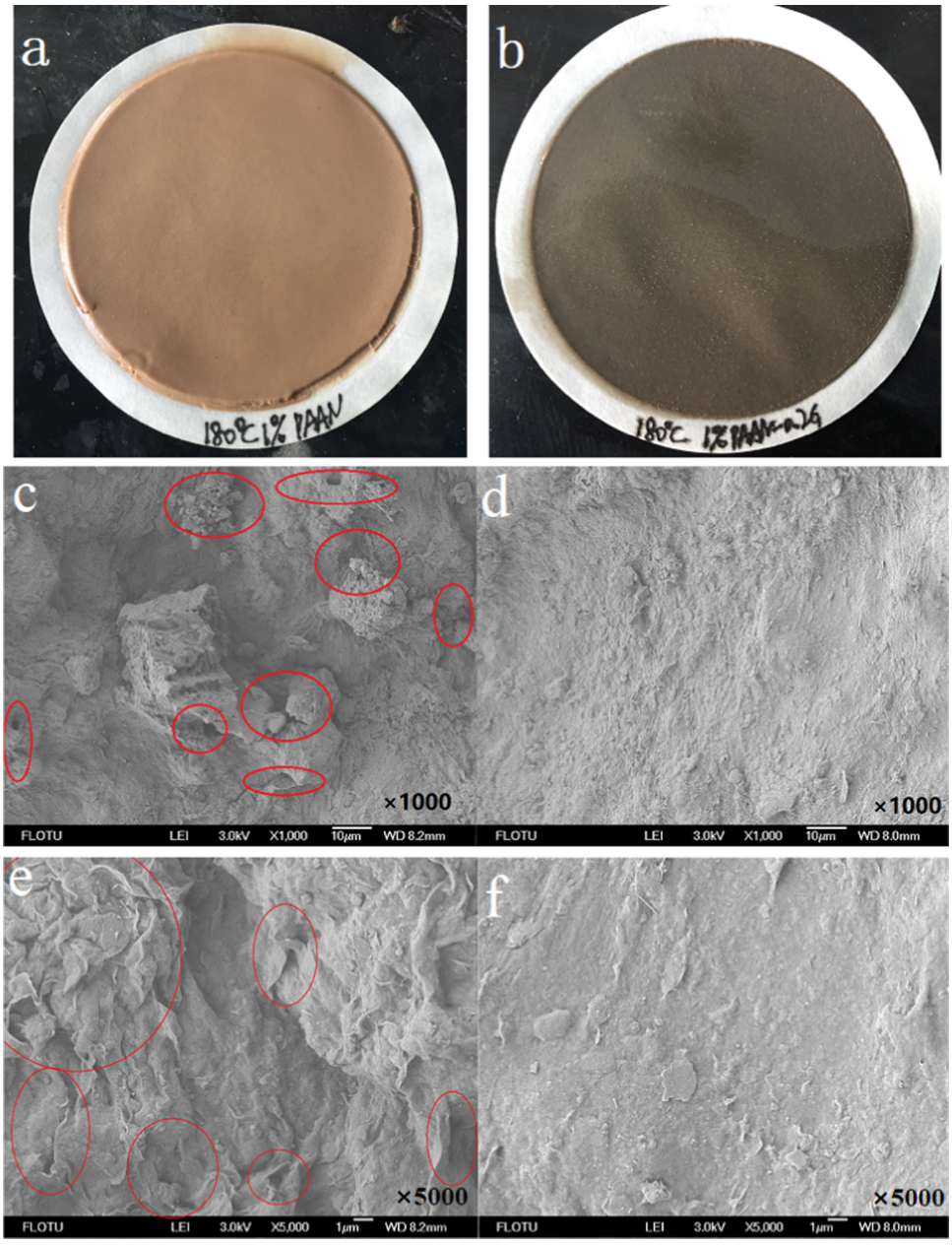

Figure 6. Filter cakes formed by the base slurry containing 1.0 wt % PAAN (a, c, e) or 1.0 wt % PAAN-0.2G (b, d, f) after aging at 180 °C. (a, b) photos and (c−f) SEM images.

that the filter cake formed by the base slurry containing 1.0 wt % PAAN had many obvious pores. Then, the filter cake containing 1.0 wt % PAAN was further enlarged 5000 times (Figure 6e), and it still showed many folds, which were formed after the fluid passed through, suggesting the noncompactness of the filter cake. However, the filter cake formed by the base slurry containing 1.0 wt % PAAN-0.2G presented a completely different morphology. It was very flat and it can be seen that there were no pores and wrinkles on the surface from the SEM image magnified 5000 times (Figure 6f), which was the reason for the lower filtration volume. The photos and SEM images of the filter cake showed that the polymer-grafted graphene oxide composite (PAAN-G) can form a thin and dense filter cake, from which not only a lower filtration volume can be obtained but also avoid the hole diameter reduction caused by the excessive thickness of the filter cake.

The particle size distribution curve (Figure 7) is a good explanation for the difference of filter cake, as shown in Figure 6. It can be seen from Figure 7a,b that the base slurry containing 1.0 wt % PAAN or 1.0 wt % PAAN-0.2G had a similar particle size distribution curve, and the difference was that the particle size distribution of the base slurry containing 1.0 wt % PAAN-0.2G was wider. Although their median particle sizes (d_{50}) are similar, the base slurry containing 1.0 wt % PAAN-0.2G had 20% of small particles below 10 μm and 6% of large particles larger than 150 μm. However, in the base slurry containing 1.0 wt % PAAN, the small particles below 10 μm accounted for only 6.5%, and almost no large particles were exceeding 150 μm. The wider particle size distribution was conducive to the effective accumulation of clay particles to form a dense filter cake. Therefore, the filter cake formed by the base slurry containing 1.0 wt % PAAN-0.2G was denser

https://doi.org/10.1021/acsomega.1c00374
ACS Omega 2021, 6, 9750−9763

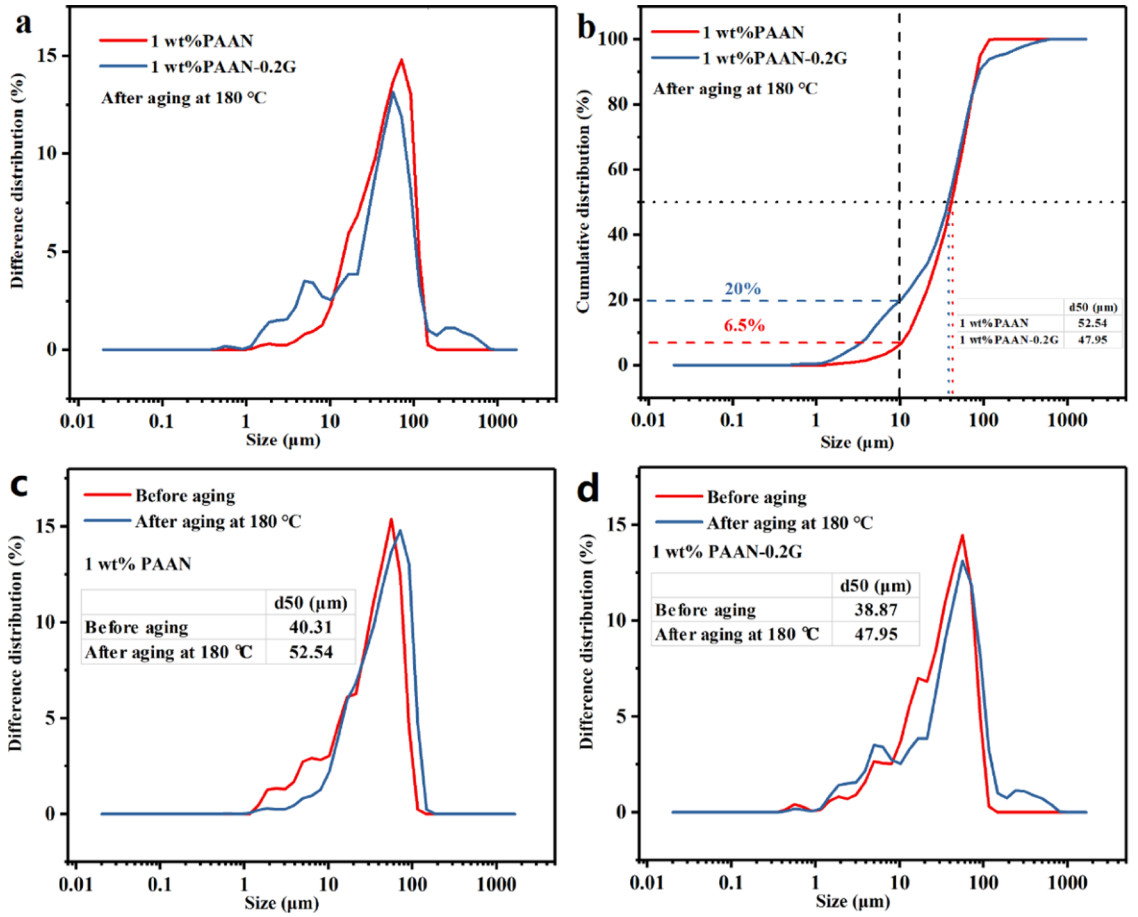

Figure 7. Particle size distribution curve of the base slurry containing 1.0 wt % PAAN or 1.0 wt % PAAN-0.2G after aging at 180 °C: (a) and (b) after aging at 180 °C; (c) 1.0 wt % PAAN before and after aging; and (d) 1.0 wt % PAAN-0.2G before and after aging.

and had low filtration volume. Figure 7c,d shows the change in the particle size distribution of 1.0 wt % PAAN and 1.0 wt % PAAN-0.2G before and after aging at 180 °C, respectively. The d_{50} values of both PAAN and PAAN-0.2G increased after aging. For 1.0 wt % PAAN, it can be clearly seen that the small particles were significantly reduced after aging, which also corresponded to the significant increase in the filtration volume at this time. On the contrary, although the d_{50} of PAAN-0.2G had also increased, its particle size distribution was still relatively uniform; the small particles had not decreased but a few large particles were added. Therefore, PAAN-0.2G could still maintain an acceptable filtration volume at this time.

The influence of concentration on the fluid loss reduction effect of PAAN-0.2G is shown in Figure 8. Before aging, increasing the concentration of PAAN-0.2G had little effect on fluid loss. After aging at 180 °C, as the concentration of PAAN-0.2G increased from 1.0 to 2.0 wt %, its API filtration volume decreased from 18 to 9.2 mL. About 2.0 wt % PAAN-0.2G can fully meet the fluid loss requirements at high temperatures, and therefore, 2.0 wt % PAAN-0.2G was used in the temperature resistance test. Figure 9 shows the comparison of the API filtration volume of the base slurry containing 2.0 wt % PAAN-0.2G or 2.0 wt % PAAN-0.5G in the temperature range 180−240 °C. Even if the aging temperature reached 240 °C, the API filtration volume of PAAN-0.2G and PAAN-0.5G was only 12.5 and 12.3 mL, indicating that both PAAN-0.2G and PAAN-0.5G can be used in ultra-high-temperature formations. Comparing the API filtration volume of PAAN-

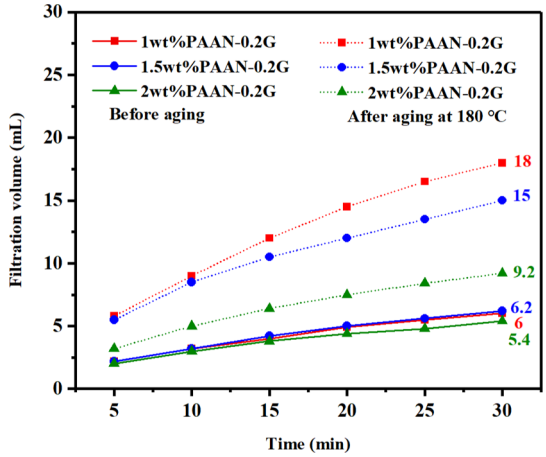

Figure 8. API filtration volume of the base slurry containing different concentrations of PAAN-0.2G before and after aging at 180 °C.

0.2G and PAAN-0.5G, it was found that the API filtration volume of the two PAAN-G at the same temperature was similar, that is, increasing the concentration of GO did not significantly enhance the fluid loss reduction capacity of PAAN-G, which may be due to the fact that the actual grafting rate of GO on PAAN did not increase significantly with the increase of GO concentration. However, the rheological properties and filtration properties of PAAN-0.2G, in this paper, in the base slurry can fully meet the actual needs of

https://doi.org/10.1021/acsomega.1c00374
ACS Omega 2021, 6, 9750−9763

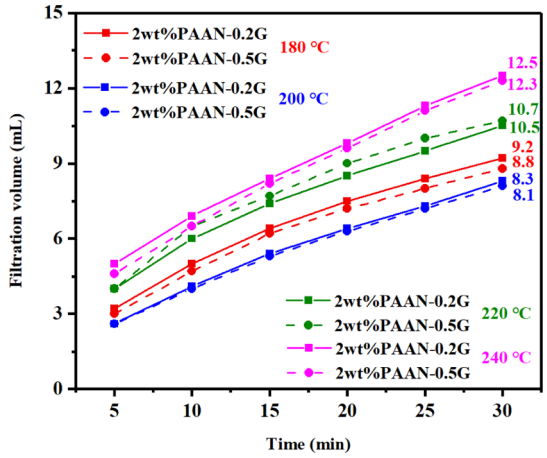

Figure 9. API filtration volume of the base slurry containing 2.0 wt % PAAN-0.2G or 2.0 wt % PAAN-0.5G at different aging temperatures.

drilling fluids. Therefore, based on cost considerations, PAAN-0.2G was the best choice as a fluid loss additive. The high-pressure and high-temperature (HP-HT) experiment further verified the temperature resistance of PAAN-0.2G. As shown in Figure 10, at a high temperature of 180−240 °C, the HP-HT

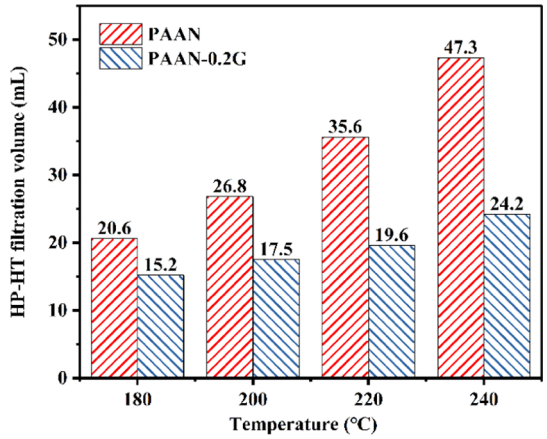

Figure 10. HP-HT filtration volume of the base slurry containing 2.0 wt % PAAN or 2.0 wt % PAAN-0.2G at different temperatures.

filtration volume of PAAN-0.2G is always lower than that of PAAN. Unlike PAAN, with the increase of temperature, the HP-HT filtration volume of PAAN-0.2G did not change significantly, indicating that PAAN-0.2G could withstand the high temperature of 240 °C.

Figure 11 shows the particle size distribution curve of the base slurry with or without 2.0 wt % PAAN-0.2G after aging at different temperatures. As the aging temperature increased, it shows the same change trend (Figure 11a,b); the particle size distribution of the slurry gradually narrowed, the small particles disappeared, and the particle size increased. When the aging temperature increased to 240 °C, the d_{50} value of the base slurry increased from 64.71 to 190.5 μm, indicating that the clay particles had undergone severe high-temperature coalescence, which was not conducive to the formation of dense filter cakes. After adding 2.0 wt % PAAN-0.2G, the d_{50} value increased from 42.04 μm at 180 °C to 70.86 μm at 240 °C. Although the particle size still increased, it was far lower than that of the base slurry.

2.4. Ability of PAAN-G to Resist Salt (NaCl) and Calcium ($CaCl_2$) Contamination. Because the surface of the colloidal plates of bentonite is negatively charged, the contamination from Na^+ and Ca^{2+} will seriously damage the diffusion double-layer structure of bentonite, which would rapidly deteriorate the rheological and filtration properties of the bentonite suspension. Figures 12 and 13 show the tolerance evaluation of PAAN-0.2G to NaCl and $CaCl_2$ at 150 °C, respectively. It can be seen from Figure 12 that the addition of 2.0 wt % PAAN-0.2G can maintain a very low API filtration volume at a NaCl concentration of up to 25.0 wt % (the API filtration volume at 30 min was 9 mL). The slope of the time-varying API filtration volume curves reflected the filtration rate (Figure 12a). When the NaCl concentration was lower than 25.0 wt %, the curves were very gentle, indicating that the filtration rate was very low and a very dense filter cake was formed. When the NaCl concentration exceeded 25.0 wt %, the API filtration volume increased sharply and the filtration rate also increased greatly. Figure 13 shows the API filtration volume changes of the base slurry containing 2.0 wt % PAAN-0.2G under different $CaCl_2$ concentrations. With the increase of $CaCl_2$ concentration from 2.0 to 5.0, 10.0, 15.0, 20.0, and 25.0 wt %, the API filtration volume gradually increased from 7.8 to 8.2, 10, 9.3, 12, 15.2 mL, respectively. Even when the concentration of $CaCl_2$ reached 25.0 wt %, its API filtration

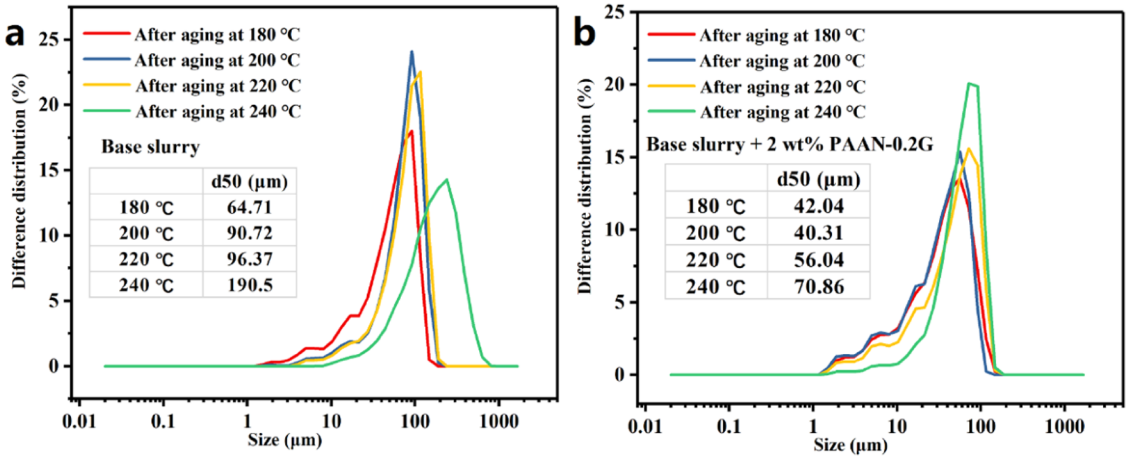

Figure 11. Particle size distribution curve of the base slurry without (a) and with (b) 2.0 wt % PAAN-0.2G after aging at different temperatures.

https://doi.org/10.1021/acsomega.1c00374
ACS Omega 2021, 6, 9750−9763

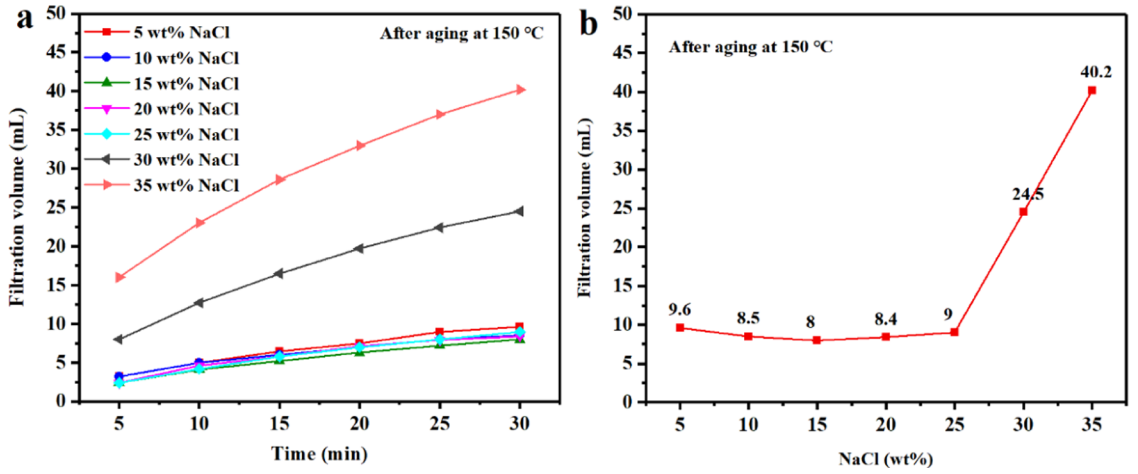

Figure 12. API filtration volume of the base slurry containing 2.0 wt % PAAN-0.2G under different NaCl concentrations: (a) filtration volume over time and (b) filtration volume for 30 min.

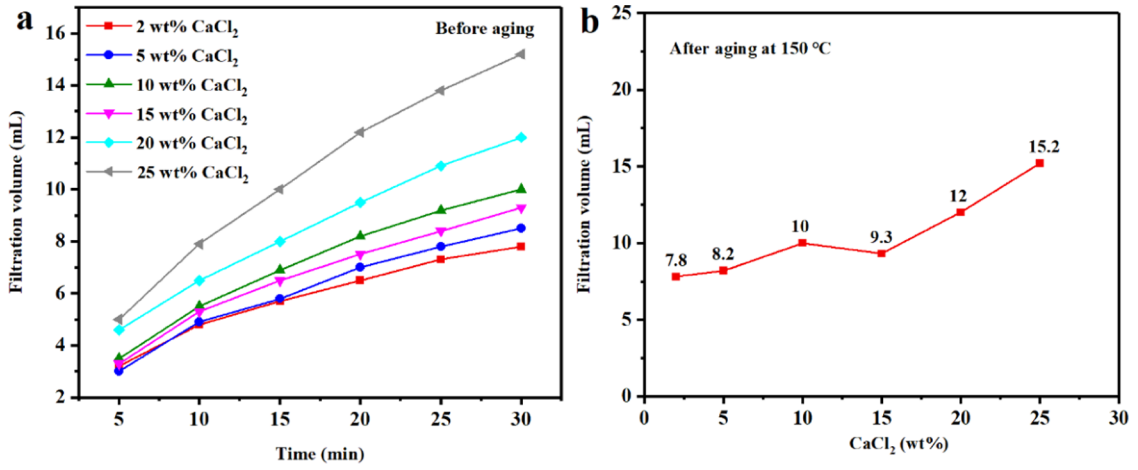

Figure 13. API filtration volume of the base slurry containing PAAN-0.2G under different $CaCl_2$ concentrations: (a) filtration volume over time and (b) filtration volume for 30 min.

volume was still within the acceptable range (Figure 13b).[21] Therefore, it can be concluded that 2.0 wt % PAAN-0.2G has excellent NaCl and $CaCl_2$ tolerance and can be used in high-salt formations.

Table 3 shows the effects of NaCl and $CaCl_2$ on the rheological properties of the base slurry containing 2 wt % PAAN-0.2G. The test was performed after aging at 150 °C. In the presence of PAAN-0.2G, the rheological parameters of the base slurry basically did not change with NaCl concentration, that is, PAAN-0.2G could keep the rheological properties of the drilling fluid stable when the NaCl concentration was lower than 25 wt %; $CaCl_2$ showed an opposite effect. Only 2 wt % of $CaCl_2$ reduced the AV of the drilling fluid from 23.5 to 6.5 mPa·s, indicating that PAAN-0.2G could not prevent $CaCl_2$ from damaging the rheological properties of the drilling fluid. However, as the concentration of $CaCl_2$ continued to increase, the rheological parameters (AV, PV, YP) of the base slurry containing 2 wt % PAAN-0.2G increased. The addition of $CaCl_2$ first destroyed the network structure formed by the clay and polymer in the fluid, and so, the fluid viscosity dropped sharply. As the concentration of $CaCl_2$ increased, the network structure was re-established between the polymer and clay and Ca^{2+}, and so, the viscosity of the fluid increased again.

Table 3. Rheological Parameters of the Base Slurry Containing 2 wt % PAAN-0.2G after Adding Different Concentrations of NaCl or $CaCl_2$ and Aging at 150 °C

	concentration (%)	AV (mPa·s)	PV (mPa·s)	YP (mPa·s)	YP/PV
NaCl	0	23.5	19	4.5	0.24
	5	25	16	9	0.56
	10	26	17	9	0.53
	15	24	15	9	0.60
	20	26	18	8	0.44
	25	25	17	8	0.47
$CaCl_2$	0	23.5	19	4.5	0.24
	2	6.5	6	0.5	0.08
	5	12.5	9	3.5	0.39
	10	13	10	3	0.30
	15	15.5	13	2.5	0.19
	20	20.5	17	3.5	0.21
	25	22.5	18	4.5	0.25

The particle size distribution curve of the salt-containing base slurry is shown in Figure 14. The particle size distribution of the base slurry remained basically unchanged after adding NaCl but changed drastically after adding $CaCl_2$. After adding $CaCl_2$, the median particle size d_{50} of the base slurry increased

https://doi.org/10.1021/acsomega.1c00374
ACS Omega 2021, 6, 9750−9763

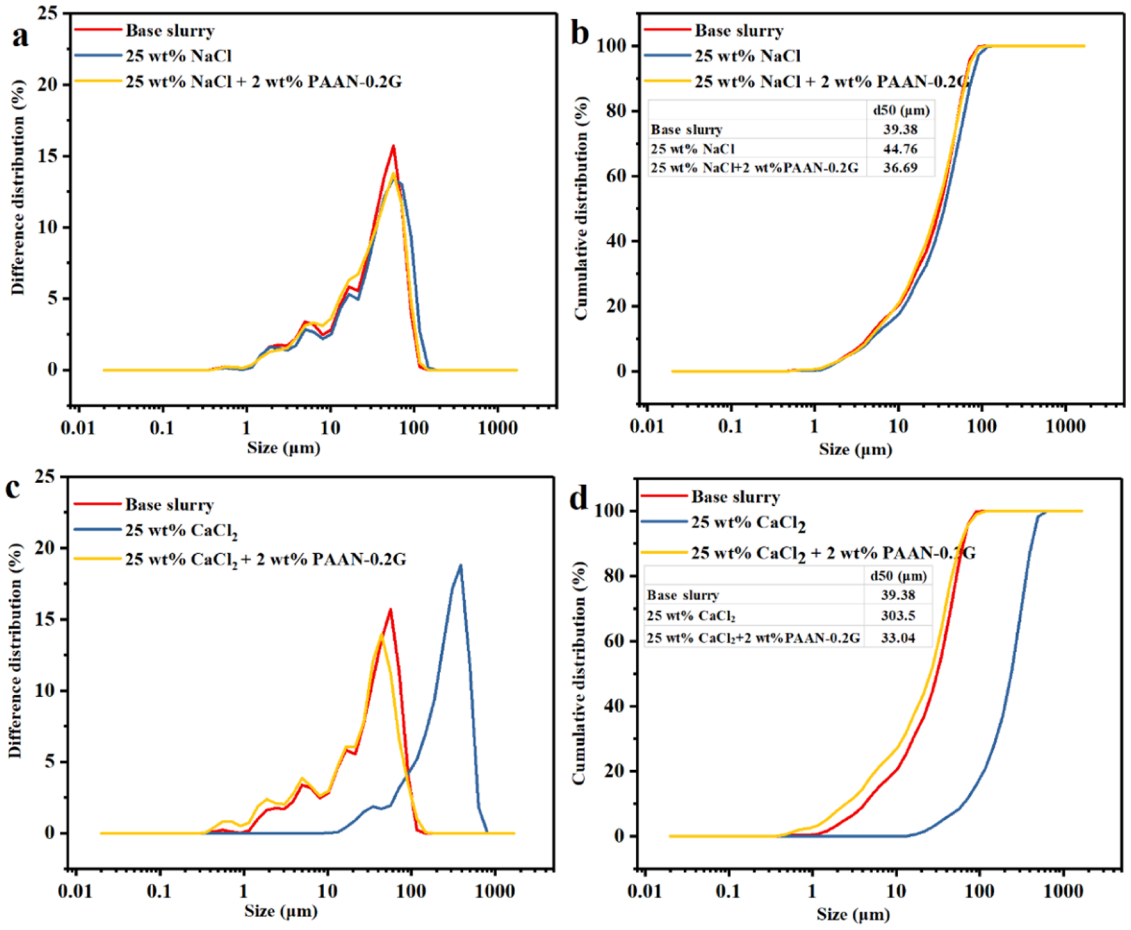

Figure 14. Particle size distribution curve of the salt-containing base slurry after aging at 150 °C: (a) and (b) NaCl; (c) and (d) $CaCl_2$.

from 39.38 to 303.5 μm, and the small particles (<10 μm) disappeared completely. This was because the hydrated cation of sodium-based montmorillonite in clay was Na^+. When Ca^{2+} was added, cation exchange occurred between the clay layers, and the thickness of the hydrated layer of Ca^{2+} was much higher than that of Na^+, so the clay particles swell sharply and the particle size increased. After adding 2 wt % PAAN-0.2G, the value of d_{50} of the base slurry containing 25 wt % $CaCl_2$ decreased from 303.5 to 33.04 μm, indicating that PAAN-0.2G can inhibit the swelling of bentonite particles caused by Ca^{2+}.

2.5. Probable Mechanism. After compositing the polymer with GO, the sulfonic acid group and the cyclic structure in the polymer chain greatly improved the temperature resistance of GO. As shown in Figure 15, the adsorption groups (amide groups, carboxyl groups, etc.) on the PAAN-G could form hydrogen bonds with oxygen atoms on the surface of bentonite, so that PAAN-G could be firmly adsorbed on the surface of bentonite. The adsorption of PAAN-G also increased the particle size distribution span of bentonite after aging. A large amount of small particle size bentonite is more conducive to filling the tiny pores and form a dense filter cake, thereby reducing the passage of water. In addition, due to the flake structure of GO, the free PAAN-G was also beneficial to insert into the tiny pores of filter cakes, all of which were conducive to improving the compactness of the filter cakes. On the other hand, the excellent resistance to Ca^{2+} contamination of PAAN-G was also attributed to the adsorption on the surface of bentonite. It was easy to exchange Ca^{2+} with Na^+ in bentonite interlayers, which caused the compression of the

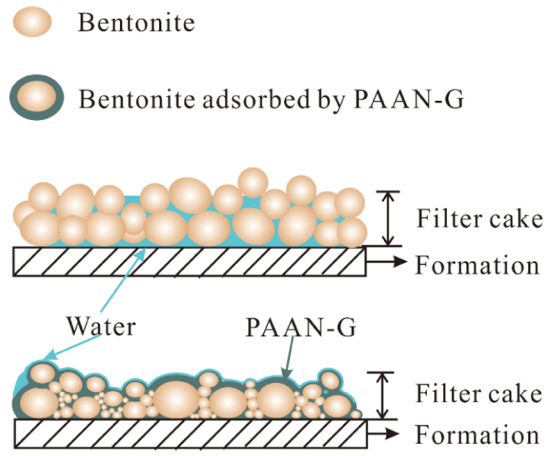

Figure 15. Schematic diagram of the mechanism of PAAN-G.

bentonite diffusion electric double layer and the aggregation of clay particles. Therefore, the filtration volume of the bentonite slurry increased greatly under Ca^{2+} contamination. The strong adsorption of PAAN-G on the surface of bentonite prevented the interlayer exchange of calcium ions, thus preventing the deterioration of filtration performance under Ca^{2+} contamination.

https://doi.org/10.1021/acsomega.1c00374
ACS Omega 2021, 6, 9750−9763

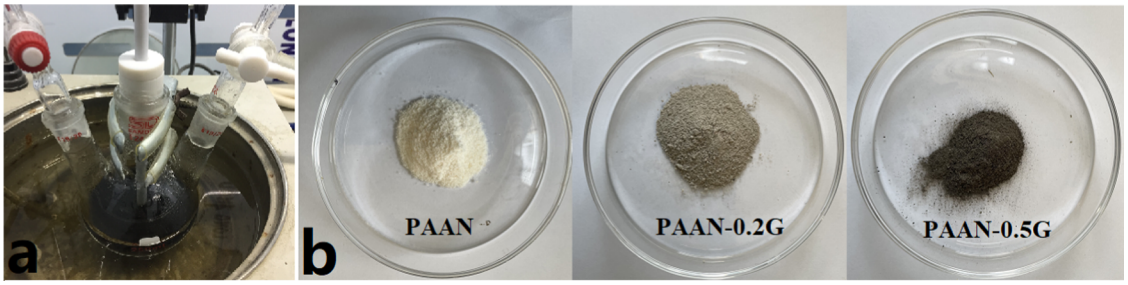

Figure 16. (a) Picture of the polymerization process and (b) the obtained powder sample.

3. CONCLUSIONS

We synthesized an acrylamide polymer/graphene oxide composite material with different GO concentrations using aqueous solution polymerization. The applicability of PAAN-G as a fluid loss additive for water-based drilling fluids under high-temperature and high-salt conditions was evaluated, and the rheological and filtration properties of bentonite-based slurry containing PAAN-G before and after high-temperature aging were studied. The chemical structure and morphology of PAAN-G were characterized by FT-IR, transmission electron microscopy (TEM), and TGA−DSC. The thermal stability of GO was greatly improved after compositing with polymer. Comparing the changes in rheological parameters and filtration volume of PAAN-0.2G and PAAN before and after aging, it was found that PAAN-0.2G can maintain stable rheological parameters after high-temperature aging, with a change rate of less than 28%. However, under the same conditions, the change rate of the rheological parameters of PAAN can reach up to 80%. Besides, the filtration volume and cake thickness of the base slurry with PAAN-0.2G were also lower than those with PAAN. PAAN-0.2G (2 wt %) can maintain a low filtration volume (12.5 mL) at 240 °C, demonstrating that PAAN-0.2G can be used in high-temperature formations. However, continuing to increase the concentration of GO in PAAN-G cannot significantly improve the rheological and filtration properties of PAAN-G in the base slurry. Based on cost considerations, PAAN-0.2G was the best choice of fluid loss additives for water-based drilling fluid. As for salt tolerance, PAAN-0.2G can maintain an acceptable filtration volume at NaCl and $CaCl_2$ concentrations as high as 25 wt %, which was enough to prove that PAAN-0.2G can be used in high-salt formations. Particle size analysis showed that PAAN-G can broaden the particle size distribution of bentonite particles in the base slurry and increase the ratio of small particles (<10 μm) and large particles (>100 μm), which helped the particles to be densely packed, resulting in forming a much thinner and denser filter cake.

4. MATERIALS AND METHODS

4.1. Materials. GO was synthesized using a modified Hummers' method from graphite powder, and the details were reported in the literature.[48,49] AM (AR, 99%), AMPS (AR, 98%), NVP (AR, 99%), ammonium persulfate (APS, AR, ≥98%), and sodium bisulfite (AR) were all commercial products from Aladdin. Sodium hydroxide (AR), sodium chloride (NaCl, AR), anhydrous calcium chloride ($CaCl_2$, AR), and other reagents were purchased from a domestic reagent company. Sodium bentonite was obtained from the Weifang Boda company. All reagents were not purified further.

4.2. Methods. *4.2.1. Synthesis of PAAN-G.* The acrylamide polymer/graphene oxide composite (PAAN-G) was prepared using the aqueous solution polymerization method.[46,50] GO (0.2 g) was added to deionized water (100 mL) and magnetically stirred at room temperature for 20 min. AM (10 g) and AMPS (15 g) were added to the GO solution and stirred magnetically to form a homogeneous solution. The pH of the solution was adjusted to 7−8 with sodium hydroxide. Then, 15 g of NVP was added. The mixed solution was poured into the reaction flask and kept in a 60 °C water bath for 30 min. Next, the initiators APS (60 mg) and sodium hydrogen persulfate (20 mg) were added to the reaction solution and then reacted at 60 °C for 2 h. The whole reaction was carried out under nitrogen protection. The polymerization process is shown in Figure 16a. The resulting product was washed and purified with absolute ethanol, then dried at 60 °C, and pulverized. The synthesis steps were repeated to prepare composite materials with 0.5 wt % GO (PAAN-0.5G) and GO-free polymers (PAAN), respectively. The synthesized GO, PAAN, and PAAN-G were dissolved in deionized water and dialyzed in deionized water for 1 week in a dialysis bag with a molecular cutoff of 3500. Then, they were redried and crushed. The obtained purified GO, PAAN, and PAAN-G were used for the physicochemical characterization of the polymer. The powder sample obtained is shown in Figure 16b.

4.2.2. Preparation of the Drilling Fluid. The base slurry was prepared by mixing 40 g of bentonite and 2.5 g of anhydrous sodium carbonate with 1000 mL of water. The suspension was stirred quickly for 20 min and then stirred at low speed and aged for 24 h at room temperature.[25] Then, different concentrations of PAAN, PAAN-0.2G, and PAAN-0.5G were added to the base slurry slowly and stirred at 6000 rpm for 20 min.

4.2.3. Performance Evaluation. A six-speed rotational viscometer (ZNN-D6S, China) was used for measuring the basic rheological parameters. The liquid was poured into the sample cup and raised to the marked line, and the readings were recorded from 600 to 300 rpm. The rheological parameters such as apparent viscosity (AV), plastic viscosity (PV), and yield point (YP) were calculated from the Ø600 (reading of 600 rpm) and Ø300 (reading of 300 rpm) values using the following formulas[50,51]

$$AV = 0.5 \cdot Ø600 \ (mPa \cdot s) \quad (1)$$

$$PV = Ø600 - Ø300 \ (mPa \cdot s) \quad (2)$$

$$YP = (2 \cdot Ø300 - Ø600)/2 \ (Pa) \quad (3)$$

The ratio of the yield point and plastic viscosity (YP/PV) is an important rheological parameter that measures the degree

https://doi.org/10.1021/acsomega.1c00374
ACS Omega 2021, 6, 9750−9763

of shear-thinning behavior of the drilling fluid. The larger the RYP, the stronger the shear-thinning behavior.[52]

The API filtration volume of the drilling fluid was determined with the MOD.SD6A medium-pressure filtration apparatus (Qingdao Haitongda Dedicated Instrument Factory, China). At room temperature, 300 mL of the drilling fluid was poured into filtration tanks, and the filtration volume was measured within 30 min after passing through a filter paper with a diameter of 9 cm at a pressure of 0.69 MPa. Then the drilling fluid was poured into an aging tank and hot-rolled at a specific temperature (150, 180, 200, 220, 240 °C) in a GW300-type variable frequency rolling furnace (Qingdao Tongchun Machinery Factory, China). The rolling time was fixed at 16 h. Rheology and API filtration tests were performed before and after the thermal aging experiments. In addition, high-pressure and high-temperature (HP-HT) filtration was also carried out at a pressure difference of 3.5 MPa and different temperatures (180, 200, 220, and 240 °C).

4.3. Characterization. *4.3.1. Fourier Transform Infrared Spectroscopy (FT-IR).* FT-IR Spectra of PAAN and PAAN-G were recorded using a Bruker FT-IR with a resolution of 4 cm^{-1} and the wavenumber range of 3600−600 cm^{-1} (Horiba, Germany). The PAAN and PAAN-G purified by dialysis were used after drying and pulverizing. The powder was placed on the sample table, compacted, and then tested.

4.3.2. Thermogravimetric Analysis (TGA). A differential thermal−thermogravimetric analyzer (TGA−DSC, METTLER TOLEDO) was used to investigate the thermal stability of PAAN, GO, and PAAN-G in a nitrogen atmosphere at a heating rate of 10 °C/min and a temperature range from 25 to 400 °C. The PAAN and PAAN-G purified by dialysis were dried, crushed, and used for TGA−DSC testing.

4.3.3. Scanning Electron Microscopy (SEM). SEM analyses were performed using a JSM7401 scanning electron microscope (JEOL, Japan). The filter cakes obtained from the filtration tests were rinsed with water to remove the floating filter cake on the surface. Then, the filter cakes were dried at 60 °C for 24 h and then cut up into squares of sizes 1.0 cm^2 × 1.0 cm^2. The dried and cut samples were adhered to conductive tapes and then metal-sprayed for 2 min.

4.3.4. Particle Size Distribution (PSD). Particle size distributions of the drilling fluid suspensions were analyzed using a Bettersize 2000 instrument. The base slurry, the base slurry containing PAAN, and the base slurry containing PAAN-G before and after aging were prepared and dispersed.[53]

AUTHOR INFORMATION

Corresponding Author

Yuxiu An − *School of Engineering and Technology, China University of Geosciences (Beijing), Beijing 100083, China; Key Laboratory of Deep Geo Drilling Technology, Ministry of Land and Resources, Beijing 100083, China;* orcid.org/0000-0002-3156-0655; Email: anyx@cugb.edu.cn

Authors

Jingyuan Ma − *School of Engineering and Technology, China University of Geosciences (Beijing), Beijing 100083, China; Key Laboratory of Deep Geo Drilling Technology, Ministry of Land and Resources, Beijing 100083, China*

Shaocong Pang − *School of Engineering and Technology, China University of Geosciences (Beijing), Beijing 100083, China; Key Laboratory of Deep Geo Drilling Technology, Ministry of Land and Resources, Beijing 100083, China*

Zenan Zhang − *School of Engineering and Technology, China University of Geosciences (Beijing), Beijing 100083, China; Key Laboratory of Deep Geo Drilling Technology, Ministry of Land and Resources, Beijing 100083, China*

Boru Xia − *School of Engineering and Technology, China University of Geosciences (Beijing), Beijing 100083, China; Key Laboratory of Deep Geo Drilling Technology, Ministry of Land and Resources, Beijing 100083, China*

Complete contact information is available at: https://pubs.acs.org/10.1021/acsomega.1c00374

Notes

The authors declare no competing financial interest.

ACKNOWLEDGMENTS

The authors would like to acknowledge the financial support from the National Natural Science Foundation of China (J218076), the National Key R&D Program of China (2016YFE0202200 and PY201802), and the Foundation of China (2-9-2018-086) for this work.

REFERENCES

(1) Li, M.-C.; Wu, Q.; Song, K.; Lee, S.; Jin, C.; Ren, S.; Lei, T. Soy Protein Isolate As Fluid Loss Additive in Bentonite-Water-Based Drilling Fluids. *ACS Appl. Mater. Interfaces* **2015**, *7*, 24799−24809.

(2) Caenn, R.; Chillingar, G. V. Drilling fluids: State of the art. *J. Pet. Sci. Eng.* **1996**, *14*, 221−230.

(3) Al-Hameedi, A. T. T.; Alkinani, H. H.; Dunn-Norman, S.; Al-Alwani, M. A.; Alshammari, A. F.; Albazzaz, H. W.; Alkhamis, M. M.; Alashwak, N. F.; Mutar, R. A. Insights into the application of new eco-friendly drilling fluid additive to improve the fluid properties in water-based drilling fluid systems. *J. Pet. Sci. Eng.* **2019**, *183*, No. 106424.

(4) Saboori, R.; Sabbaghi, S.; Kalantariasl, A. Improvement of rheological, filtration and thermal conductivity of bentonite drilling fluid using copper oxide/polyacrylamide nanocomposite. *Powder Technol.* **2019**, *353*, 257−266.

(5) Agwu, O. E.; Akpabio, J. U. Using agro-waste materials as possible filter loss control agents in drilling muds: A review. *J. Pet. Sci. Eng.* **2018**, *163*, 185−198.

(6) Akpan, E. U.; Enyi, G. C.; Nasr, G.; Yahaya, A. A.; Ahmadu, A. A.; Saidu, B. Water-based drilling fluids for high-temperature applications and water-sensitive and dispersible shale formations. *J. Pet. Sci. Eng.* **2019**, *175*, 1028−1038.

(7) Yuxiu, A.; Jiang, G.; Qi, Y.; Huang, X.; Shi, H. High-performance shale plugging agent based on chemically modified graphene. *J. Nat. Gas. Sci. Eng.* **2016**, *32*, 347−355.

(8) Feng, Q.; Liu, H.; Peng, Z.; Zheng, Y. Synthesis, characterization and evaluation of long-acting hyperbranched cationic polymer clay stabilizer used in water flooding. *Polym. Test.* **2020**, *82*, No. 106344.

(9) Chu, Q.; Lin, L.; Zhao, Y. Hyperbranched polyethylenimine modified with silane coupling agent as shale inhibitor for water-based drilling fluids. *J. Pet. Sci. Eng.* **2019**, *182*, No. 106333.

(10) Xie, G.; Xiao, Y.; Deng, M.; Luo, Y.; Luo, P. Low Molecular Weight Branched Polyamine as a Clay Swelling Inhibitor and Its Inhibition Mechanism: Experiment and Density Functional Theory Simulation. *Energy Fuels* **2020**, *34*, 2169−2177.

(11) Bailey, L.; Boek, E. S.; Jacques, S. D. M.; Boassen, T.; Selle, O. M.; Argillier, J. F.; Longeron, D. G. Particulate Invasion From Drilling Fluids. *SPE Journal* **2000**, *5*, 412−419.

(12) Ba geri, B. S.; Mahmoud, M.; Elkatatny, S.; Patil, S.; Benaafi, M.; Mohamed, A. In *Effect of Drill Cuttings Mechanical Properties on Filter Cake Properties and Mud-Filtrate Invasion*, 53rd U.S. Rock Mechanics/Geomechanics Symposium, 2019.

(13) Sepehri, S.; Soleyman, R.; Varamesh, A.; Valizadeh, M.; Nasiri, A. Effect of synthetic water-soluble polymers on the properties of the

heavy water-based drilling fluid at high pressure-high temperature (HPHT) conditions. *J. Pet. Sci. Eng.* **2018**, *166*, 850−856.
(14) Cao, J.; Meng, L.; Yang, Y.; Zhu, Y.; Wang, X.; Yao, C.; Sun, M.; Zhong, H. Novel Acrylamide/2-Acrylamide-2-methylpropanesulfonic Acid/4-Vinylpyridine Terpolymer as an Anti-calcium Contamination Fluid-Loss Additive for Water-Based Drilling Fluids. *Energy Fuels* **2017**, *31*, 11963−11970.
(15) Navarrete, R. C.; Himes, R. E.; Seheult, J. M. In *Applications of Xanthan Gum in Fluid-Loss Control and Related Formation Damage*, SPE Permian Basin Oil and Gas Recovery Conference; Society of Petroleum Engineers: Midland, Texas, 2000; p 21.
(16) Zhou, G.; Qiu, Z.; Zhong, H.; Zhao, X.; Kong, X. Study of Environmentally Friendly Wild Jujube Pit Powder as a Water-Based Drilling Fluid Additive. *ACS Omega* **2021**, *6*, 1436−1444.
(17) Li, X.; Jiang, G.; Shen, X.; Li, G. Application of Tea Polyphenols as a Biodegradable Fluid Loss Additive and Study of the Filtration Mechanism. *ACS Omega* **2020**, *5*, 3453−3461.
(18) Nasiri, A.; Ameri Shahrabi, M. J.; Sharif Nik, M. A.; Heidari, H.; Valizadeh, M. Influence of monoethanolamine on thermal stability of starch in water based drilling fluid system. *Pet. Explor. Dev.* **2018**, *45*, 167−171.
(19) Dias, F. T. G.; Souza, R. R.; Lucas, E. F. Influence of modified starches composition on their performance as fluid loss additives in invert-emulsion drilling fluids. *Fuel* **2015**, *140*, 711−716.
(20) Zhong, H.; Kong, X.; Chen, S.; Grady, B. P.; Qiu, Z. Preparation, characterization and filtration control properties of crosslinked starch nanospheres in water-based drilling fluids. *J. Mol. Liq.* **2021**, *325*, No. 115221.
(21) Li, M.-C.; Wu, Q.; Song, K.; De Hoop, C. F.; Lee, S.; Qing, Y.; Wu, Y. Cellulose Nanocrystals and Polyanionic Cellulose as Additives in Bentonite Water-Based Drilling Fluids: Rheological Modeling and Filtration Mechanisms. *Ind. Eng. Chem. Res.* **2016**, *55*, 133−143.
(22) Li, M.-C.; Wu, Q.; Song, K.; Qing, Y.; Wu, Y. Cellulose Nanoparticles as Modifiers for Rheology and Fluid Loss in Bentonite Water-based Fluids. *ACS Appl. Mater. Interfaces* **2015**, *7*, 5006−5016.
(23) Ma, J. Y.; Xia, B. R.; Yu, P. Z.; An, Y. X. Comparison of an Emulsion- and Solution-Prepared Acrylamide/AMPS Copolymer for a Fluid Loss Agent in Drilling Fluid. *ACS Omega* **2020**, *5*, 12892−12904.
(24) He, J.; Chen, Q. M.; Zhao, W.; Chen, F.; Wang, W. L. Hydrophobically modified cationic oligoacrylamide as a potential shale hydration inhibitor in water-based drilling fluid and mechanism study. *J. Nat. Gas Sci. Eng.* **2020**, *81*, No. 103484.
(25) Ma, J.; Xia, B.; Yu, P.; An, Y. Comparison of an Emulsion- and Solution-Prepared Acrylamide/AMPS Copolymer for a Fluid Loss Agent in Drilling Fluid. *ACS Omega* **2020**, *5*, 12892−12904.
(26) Hamad, B. A.; He, M.; Xu, M.; Liu, W.; Mpelwa, M.; Tang, S.; Jin, L.; Song, J. A Novel Amphoteric Polymer as a Rheology Enhancer and Fluid-Loss Control Agent for Water-Based Drilling Muds at Elevated Temperatures. *ACS Omega* **2020**, *5*, 8483−8495.
(27) Beg, M.; Sharma, S.; Ojha, U. Effect of cationic copolyelectrolyte additives on drilling fluids for shales. *J. Pet. Sci. Eng.* **2018**, *161*, 506−514.
(28) Luo, Z.; Pei, J.; Wang, L.; Yu, P.; Chen, Z. Influence of an ionic liquid on rheological and filtration properties of water-based drilling fluids at high temperatures. *Appl. Clay. Sci.* **2017**, *136*, 96−102.
(29) Wang, K.; Jiang, G.; Liu, F.; Yang, L.; Ni, X.; Wang, J. Magnesium aluminum silicate nanoparticles as a high-performance rheological modifier in water-based drilling fluids. *Appl. Clay. Sci.* **2018**, *161*, 427−435.
(30) Minakov, A. V.; Mikhienkova, E. I.; Voronenkova, Y. O.; Neverov, A. L.; Zeer, G. M.; Zharkov, S. M. Systematic experimental investigation of filtration losses of drilling fluids containing silicon oxide nanoparticles. *J. Nat. Gas. Sci. Eng.* **2019**, *71*, No. 102984.
(31) Perween, S.; Thakur, N. K.; Beg, M.; Sharma, S.; Ranjan, A. Enhancing the properties of water based drilling fluid using bismuth ferrite nanoparticles. *Colloids Surf., A* **2019**, *561*, 165−177.
(32) Beg, M.; Kumar, P.; Choudhary, P.; Sharma, S. Effect of high temperature ageing on TiO2 nanoparticles enhanced drilling fluids: A rheological and filtration study. *Upstream Oil and Gas Technol.* **2020**, *5*, No. 100019.
(33) Cai, J.; Chenevert, M. E.; Sharma, M. M. In *Friedheim J. Decreasing Water Invasion into Atoka Shale Using Non-modified Silica Nanoparticles*, SPE Annual Technical Conference and Exhibition; Society of Petroleum Engineers: Denver, Colorado, USA, 2011; p 12.
(34) Sensoy, T.; Chenevert, M. E.; Sharma, M. M. In *Minimizing Water Invasion in Shales Using Nanoparticles*, SPE Annual Technical Conference and Exhibition; Society of Petroleum Engineers: New Orleans, Louisiana, 2009.
(35) Zhang, Q.; Zhou, J-s.; Zhai, Y-a.; Liu, F-q.; Gao, G. Effect of salt solutions on chain structure of partially hydrolyzed polyacrylamide. *J. Cent. South Univ. Technol.* **2008**, *15*, 80−83.
(36) Seright, R. S. S.; Campbell, A.; Mozley, P.; Han, P. Stability of Partially Hydrolyzed Polyacrylamides at Elevated Temperatures in the Absence of Divalent Cations. *SPE J.* **2010**, *15*, 341−348.
(37) Mao, H.; Qiu, Z.; Shen, Z.; Huang, W. Hydrophobic associated polymer based silica nanoparticles composite with core−shell structure as a filtrate reducer for drilling fluid at utra-high temperature. *J. Pet. Sci. Eng.* **2015**, *129*, 1−14.
(38) An, Y.; Jiang, G.; Qi, Y.; Ge, Q.; Zhang, L. Nano-fluid loss agent based on an acrylamide based copolymer "grafted" on a modified silica surface. *Rsc Adv.* **2016**, *6*, 17246−17255.
(39) Rana, A.; Khan, I.; Ali, S.; Saleh, T. A.; Khan, S. A. Controlling Shale Swelling and Fluid Loss Properties of Water-Based Drilling Mud via Ultrasonic Impregnated SWCNTs/PVP Nanocomposites. *Energy Fuels* **2020**, *34*, 9515−9523.
(40) Oseh, J. O.; Mohd Norddin, M. N. A.; Ismail, I.; Gbadamosi, A. O.; Agi, A.; Mohammed, H. N. A novel approach to enhance rheological and filtration properties of water−based mud using polypropylene−silica nanocomposite. *J. Pet. Sci. Eng.* **2019**, *181*, No. 106264.
(41) Wu, Q.; Xu, Y.; Yao, Z.; Liu, A.; Shi, G. Supercapacitors Based on Flexible Graphene/Polyaniline Nanofiber Composite Films. *Acs Nano* **2010**, *4*, 1963−1970.
(42) Xu, Y.; Bai, H.; Lu, G.; Li, C.; Shi, G. Flexible graphene films via the filtration of water-soluble noncovalent functionalized graphene sheets. *J. Am. Chem. Soc.* **2008**, *130*, 5856−5857.
(43) Kosynkin, D. V.; Ceriotti, G.; Wilson, K. C.; Lomeda, J. R.; Scorsone, J. T.; Patel, A. D.; Friedheim, J. E.; Tour, J. M. Graphene Oxide as a High-Performance Fluid-Loss-Control Additive in Water-Based Drilling Fluids. *ACS Appl. Mater. Interfaces* **2012**, *4*, 222−227.
(44) Yuxiu, A.; Guancheng, J.; Yourong, Q.; Xianbin, H.; He, S. High-performance shale plugging agent based on chemically modified graphene. *J. Nat. Gas. Sci. Eng.* **2016**, *32*, 347−355.
(45) Aramendiz, J.; Imqam, A. Water-based drilling fluid formulation using silica and graphene nanoparticles for unconventional shale applications. *J. Pet. Sci. Eng.* **2019**, *179*, 742−749.
(46) Gudarzifar, H.; Sabbaghi, S.; Rezvani, A.; Saboori, R. Experimental investigation of rheological & filtration properties and thermal conductivity of water-based drilling fluid enhanced. *Powder Technol.* **2020**, *368*, 323−341.
(47) Zhang, N.; Li, R.; Zhang, L.; Chen, H.; Wang, W.; Liu, Y.; Wu, T.; Wang, X.; Wang, W.; Li, Y.; Zhao, Y.; Gao, J. Actuator materials based on graphene oxide/polyacrylamide composite hydrogels prepared by in situ polymerization. *Soft Matter* **2011**, *7*, 7231.
(48) Hummers, W. S.; Offeman, R. E. Preparation of Graphitic Oxide. *J. Am. Chem. Soc.* **1958**, *80*, 1339.
(49) Xu, Y.; Zhao, L.; Bai, H.; Hong, W.; Li, C.; Shi, G. Chemically Converted Graphene Induced Molecular Flattening of 5,10,15,20-Tetrakis(1-methyl-4-pyridinio)porphyrin and Its Application for Optical Detection of Cadmium(II) Ions. *J. Am. Chem. Soc.* **2009**, *131*, 13490−13497.
(50) Ma, J.; An, Y.; Yu, P. Core-shell structure acrylamide copolymer grafted on nano-silica surface as an anti-calcium and anti-temperature fluid loss agent. *J. Mater. Sci.* **2019**, *54*, 5927−5941.
(51) Chu, Q.; Lin, L. Effect of molecular flexibility on the rheological and filtration properties of synthetic polymers used as fluid loss additives in water-based drilling fluid. *Rsc Adv.* **2019**, *9*, 8608−8619.

https://doi.org/10.1021/acsomega.1c00374
ACS Omega 2021, 6, 9750−9763

(52) Okrajni, S.; Azar, J. J. The Effects of Mud Rheology on Annular Hole Cleaning in Directional Wells. *SPE Drilling Engineering* **1986**, *1*, 297−308.
(53) Ma, J.; Yu, P.; Xia, B.; An, Y. Micro-manganese as a weight agent for improving the suspension capability of drilling fluid and the study of its mechanism. *Rsc Adv.* **2019**, *9*, 35509−35523.

https://doi.org/10.1021/acsomega.1c00374
ACS Omega 2021, 6, 9750−9763